Proceedings of the Thirty-second (2022) International Ocean and Polar Engineering Conference **www.isope.org**
Shanghai, China, June 5–10, 2022

ISBN 978-1-880653-81-4; ISSN 1098-6189

Comparative Study on Wake Instabilities of a Propeller with and without Duct

Xidi Zhang[1], Jianwei Wu[2], Liushuai Cao[1], Decheng Wan[1]*

[1] Computational Marine Hydrodynamics Lab (CMHL), School of Naval Architecture, Ocean and Civil Engineering, Shanghai Jiao Tong University, Shanghai, China
[2] Wuhan Second Ship Design and Research Institute, Wuhan, China
*Corresponding author

ABSTRACT

Due to its special geometric shape and appropriate propeller and duct design, ducted propeller has the characteristics of low noise, high efficiency, and ability to work normally under heavy load conditions, which are superior to ordinary propellers. The existence of the duct has a significant impact on the open water performance, vortex structures, as well as the instability of the wake evolution. In this paper, based on the Ka4-70 propeller and 19A duct model, simulations of open water propeller and a ducted propeller with tip clearance d = 1.01mm are carried out. Firstly, open water simulations of the two conditions were performed. Numerical results of d=1.01mm ducted propeller were compared with the experimental data to verify the accuracy of the simulation. Four sets of meshes with different resolution and density were used to undertake the grid independence study. Secondly, based on the detached eddy simulation (DES) turbulence modelling method, three advance coefficients J = 0.2, 0.6 and 1.0 were simulated. The influence of the duct on vortex structures was analyzed in detail. The measurement points were set at y/R = 0.9, x/R = 0.25, 1.5, 3.6, and 6, of which the flow field scalars were collected for spectrum analysis. Results show that the existence of the duct has a significant effect on the wake structures of the propeller.

KEY WORDS: ducted propeller; wake; instability; DES; tip clearance

INTRODUCTION

Ducted propeller is one of the special propellers. Compared with the open water propeller, it has an external duct, and propeller is fixed in the middle of duct with a two-dimensional hydrofoil in cross-section. In general applications in the marine propulsion field, the results show that duct can improve propeller's thrust and torque and other propulsion parameters, and can provide additional thrust under heavy load and low speed conditions, thereby improving the propulsion efficiency of the ducted propeller in given conditions. In addition, the duct also has a significant optimization effect on the propeller flow field. The propeller wake working behind ship has been significantly improved, so the main engine power can be absorbed under some working conditions. At the same time, it has been found in recent studies by Wang et al. (2019) and Qin et al. (2021) that when the ducted propeller is arranged on a heavy-duty ship, it is beneficial to reduce vibration, which is helpful to improve the noise performance. In addition, with the development of underwater unmanned vehicles, ducted propellers have been widely used due to their resistance is in general increased to external sea conditions, anti-interference ability to maintain a stable heading, and protection of the propeller to deal with complex underwater conditions. However, if rubbish is sucked, the resistance performance is just worse, which is a major disadvantage of the ducted propeller.

The hydrodynamic performance of ducted propellers is affected by many factors. Research on ducted propellers generally adopts changing a single parameter to observe its influence on various performances of ducted propellers. Among them, Gaggero et al. (2017) studies explored its influence on the hydrodynamic performance of the ducted propeller by using different ducts, and Song et al. (2015) explored its influence on the hydrodynamic performance of the ducted propeller by changing the geometric parameters of the propeller such as the propeller shaft and the disk surface ratio. Compared with open-water propellers, ducted propellers have many special properties, and the flow characteristics of the flow field and the dynamics of wakes are also quite different from those of open-water propellers. There are few comparisons such as the study of Gong et al. (2021) between ducted propellers and open water propellers.

There are some related researches on the analysis and research of propeller wake instability in China. Wang et al. (2021) carried out numerical and experimental studies on the dynamic characteristics of the propeller wake based on the delayed detached eddy simulation (DDES), large eddy simulation (LES) and non-turbulence model simulation methods, and particle image velocity measurement flow field test, respectively, the triggering mechanism of propeller wake instability is analyzed.

Heydari et al. (2020) used computational fluid dynamics (CFD) numerical simulation methods to study the wake field behind the propeller under different propulsion coefficients under open water conditions. The local variables (velocity, pressure) and wake structure characteristics are extensively analyzed using mean analysis, root mean square analysis and Fourier analysis. When the advance coefficient J is high, the rotation of the entire propeller determines the fluctuation of the side force, and when the advance coefficient J is low, the rotation of a

single blade mainly affects the side force.
Wang et al. (2019) analyzed the wake dynamics characteristics of the front rudder propeller under open water conditions, and studied the evolution mechanism of the wake under different propulsion coefficients and rudder angles. The interaction between the wake and the rudder increases as the advancement coefficient increases, resulting in more complex topology of the vortex system. Through the analysis of the kinetic energy (KE) and pressure spectrum of the rudder surface, the evolution of the vortex structure is further analyzed.
Qin et al. (2021) used DES method to numerically analyze the wake vortex instability of the pre-rotation pump jet thruster. The results show that when the advance coefficient *J* is low, the tip vortex appears a unique multi-induction unstable mode, which is called the "pre-stack" phenomenon. The study found that the instability of the tip vortex is not only related to the distance between the spirals, but also related to the highest efficiency point of the propeller. The unstable starting point of the tip vortex moves downstream with the increase of *J*. When *J* is greater than the highest efficiency point of the propeller, the stable length of the tip vortex drops sharply. The energy transfer process from the blade subharmonic of the tip vortex to the axial subharmonic depends on *J*, and is related to the spatial evolution of the tip vortex.
Li et al. (2021) used the mixed stress vortex simulation method to study the wake of a pump jet thruster with a pre-rotating stator. Through the systematic comparison of wake morphology under different load conditions, the flow field is analyzed in detail, and the wake instability process and instability mechanism are investigated. The tip clearance leakage vortex is first manifested as short-wave instability. Under the action of the duct shedding vortex, the unstable process of the leakage vortex is accelerated, which promotes the generation of the secondary vortex. The secondary vortex further enhances the instability process and leads to the evolution of chaos.
Felli et al. (2011) experimentally studied the evolution mechanism of the propeller tip and hub vortex in the transition zone and the far field. The experiment includes detailed time-resolved visualization and velocity measurement. The purpose is to examine the influence of spiral-spiral distance on wake evolution and unstable transition mechanism. Studies have shown that this phenomenon is driven by the mutual inductance between adjacent spirals, and the characteristics of the mutual inductance change with the number of blades.
The research on ducted propellers has a long history (Hughes et al.,1992), especially after the rapid development of computational fluid dynamics. However, the focus of these studies is more on the efficiency and hydrodynamic performance of the ducted propeller, and there is less research on the influence mechanism of the duct. The duct has a significant influence on its hydrodynamic performance, the pressure and velocity distribution characteristics of the wake field, etc. In addition, the wake instability of the ducted propeller has a significant impact on its noise and wake dynamics. Compared with conventional propellers, the existence of ducts makes the wake instability of ducted propellers have different development laws. The mechanism analysis of the influence mechanism of the duct on the wake instability has far-reaching guiding significance for the optimization of the hydrodynamic performance and noise performance of the ducted propeller, and can provide a reference for the design of the ducted propeller.
The chapters of this article are arranged as follows: Firstly, open water simulations of the two conditions were performed. Numerical results of ducted propeller were compared with the experimental data to verify the accuracy of the simulation. Four sets of meshes with different resolution and density were used to undertake the grid independence study. Secondly, based on the detached eddy simulation (DES) turbulence modelling method, three advance coefficients *J* =0.2, 0.6 and 1.0 were simulated. The influence of the duct on vortex structures was analyzed in detail. The measurement points were set at *y/R* = 0.9, *x/R* = 0.25, 1.5, 3.6, and 6, in order to explore the wake instability of propeller, and the vortices shed by propellers are located in this areas, of which the flow field scalars were collected for spectrum analysis.

NUMERICAL METHOD

The duct is placed around the propeller. In its selection, the research in this paper is based on Ka4-70 propeller and 19A duct, using the same working conditions, namely, the advance coefficient *J*=0.2, 0.6 and 1.0, to simulate open water propeller and ducted propeller. The tip clearance *d* is based on the literature by Carlo (2015). Take *d* = 1.01mm, which means that the gap-to-diameter ratio *GSR*=0.46%.
Propeller modeling is carried out in CATIA, and the geometric model obtained is shown in Fig.1:

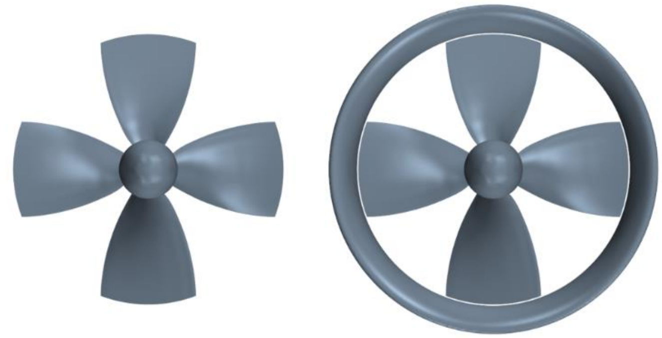

Fig.1 Geometry model of non-ducted and ducted propeller

Turbulence model

The SST *k-ω* model was proposed by Menter (1993, 1994) and has been continuously developed. For the calculation of the convective decompression zone, the *k-ω* model is more suitable because of the vigorous propeller tail flow and near wall flow. The *k-ω* model also takes the orthogonal divergence term into account, which expands its scope of application to make it both in the near wall and the far wall applies. The SST *k-ω* flow equations are as follows:

$$\frac{\partial}{\partial x_i}(\rho k u_i)+\frac{\partial}{\partial t}(\rho k)=\frac{\partial}{\partial x_j}\left(\Gamma_k\frac{\partial k}{\partial x_j}\right)+P_k-D_k \tag{1}$$

$$\frac{\partial}{\partial x_i}(\rho \omega u_i)+\frac{\partial}{\partial t}(\rho \omega)=\frac{\partial}{\partial x_j}\left(\Gamma_\omega\frac{\partial \omega}{\partial x_j}\right)+P_\omega-D_\omega+O_\omega \tag{2}$$

k is the turbulent kinetic energy; ω is the specific dissipation of the turbulent kinetic energy. P_k and P_ω are the production of kinetic energy and ω; D_k and D_ω are the dissipation of kinetic energy. Γ_k and Γ_ω are the effective diffusion term of k and ω; O_ω represents the orthogonal divergence term.

The LES and RANS hybrid method combines the advantages of the two methods, namely, RANS method is employed in the boundary layer, and LES is used in vortex shedding areas (Cao et al.,2021). DES method is a typical representative method among them. Spalart et al. (2006) use the same mathematical characteristics of the governing equations of LES and RANS, the unified governing equations are adopted, and only mixing functions are added to the equations or some source terms in the equations are changed to realize the conversion between different methods. For example, the momentum equation under incompressible conditions can be written as:

$$\frac{1}{\rho}\frac{\partial\tilde{p}}{\partial x_i}+\frac{\partial\tilde{u}_i}{\partial t}+\tilde{u}_j\frac{\partial\tilde{u}_i}{\partial x_j}-v\frac{\partial^2\tilde{u}_i}{\partial x_j^2}=-\frac{\partial\left(f^{RANS}\tau_{ij}^{RANS}+f^{LES}\tau_{ij}^{LES}\right)}{\partial x_j} \tag{3}$$

In the above formula, τ_{ij}^{RANS} and τ_{ij}^{LES} represent the Reynolds stress and the sublattice stress, respectively, in the RANS and LES methods, f^{RANS} and f^{LES} are the control coefficients.

Open Water Performance

Using Siemens STARCCM+ software to carry out the simulation, the final calculation mesh number is set to 5.2 million (without duct) about 7.6 million (with 19A duct). The thrust coefficient K_T, thruster efficiency η_0 and torque coefficient K_Q is obtained by the obtained data such as the thrust, torque and lateral force in the data processing of related hydrodynamic forces. Furthermore, the dimensionless coefficients more intuitively express the changing laws of the corresponding physical quantities, and are necessary methods and means for later data processing and result analysis. It plays a vital role in propeller open water test and CFD simulation. Among them, the commonly used performance parameters and calculation formulas of ducted propellers are as follows:

$$K_{TB} = \frac{T_B}{\rho n^2 D^4} \tag{4}$$

$$K_{TD} = \frac{T_D}{\rho n^2 D^4} \tag{5}$$

$$K_Q = \frac{Q_B}{\rho n^2 D^5} \tag{6}$$

$$K_T = K_{TB} + K_{TD} \tag{7}$$

$$J = \frac{V_{in}}{nD} \tag{8}$$

$$\eta_0 = \frac{J}{2\pi}\frac{K_T}{K_Q} \tag{9}$$

Among them, T_B is the blade thrust, T_D is the duct thrust, and Q_B is the blade torque, ρ is the water density. K_{TB} and K_{TD} are the propeller thrust coefficient and duct thrust coefficient respectively, K_T represents the total thrust coefficient of the ducted propeller, K_Q is the propeller torque coefficient, η_0 represents the efficiency of the ducted propeller, n is the rotation rate, and D is the propeller diameter.

VALIDATION AND VERIFICATION

In order to verify the mesh convergence of the simulation method, four sets of meshes with different densities were used to simulate the Ka4-70 19A ducted propeller with d = 1.01mm and the results were compared. Their blade meshes are shown in Fig.2.The four sets of meshes range from sparse to dense, namely, the total mesh number is 0.2 million in Fig.2(a), 0.7 million in (b), 2.7 million in (c), and 7.6 million in (d).

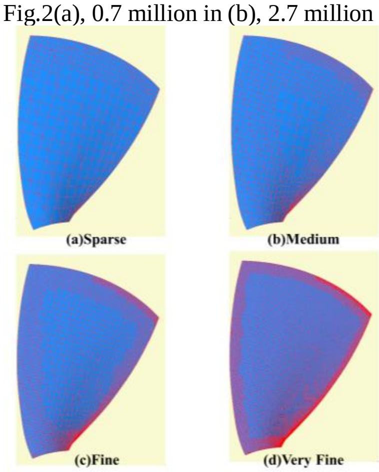

Fig.2 Four blade meshes of ducted propeller

The setting of the boundary conditions is shown in the figure below. The inlet is set as the speed inlet, the outlet is set as the pressure outlet, and the remaining boundary surfaces are set as symmetrical planes to simulate the situation of infinite water.

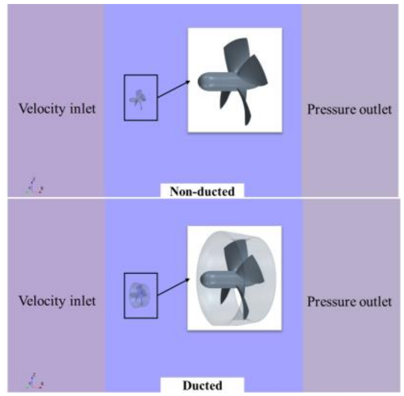

Fig.3 Boundary conditions of non-ducted and ducted propeller

To verify mesh convergence of the simulation method, four sets of mesh with different densities were used to simulate the Ka4-70 19A ducted propeller with d = 1.01mm and the results were compared. The four sets of mesh range from sparse to dense.
The relative reference frame method and the SST k-ω turbulence model are adopted, and the advance coefficient J = 0.6, which is the most commonly used advance coefficient for the ducted propeller efficiency. Four groups of ducted propellers with different density meshes are simulated, and the hydrodynamic performance data of ducted propellers, such as thrust and torque, are obtained. The following is the result of dimensionless open water performance coefficient.
The results show that as the number of grids increases, the hydrodynamic performance coefficients gradually converge to the experimental values, and the errors are all within 5%, which shows that the simulation is feasible and accurate. Moreover, the mesh convergence verification was carried in our paper by Zhang et al. (2021).

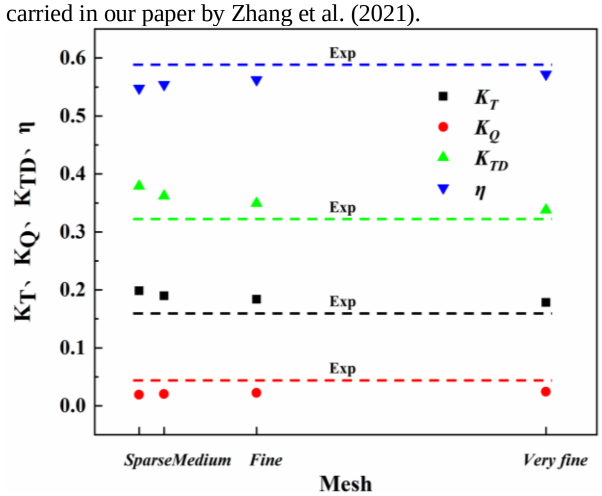

Fig.4 Open water performance results of four meshes duct propellers

In order to better simulate the flow of the propeller wake tip vortex, the ducted propeller duct and the blade tip clearance, the above-mentioned area was refined to obtain the grid as shown in Fig.5 and Fig.6. Namely, Fig.5 is a comparison of longitudinal section grids with and without ducts, and Fig.6 is the mesh side view at the duct and the tip clearance of ducted propeller.

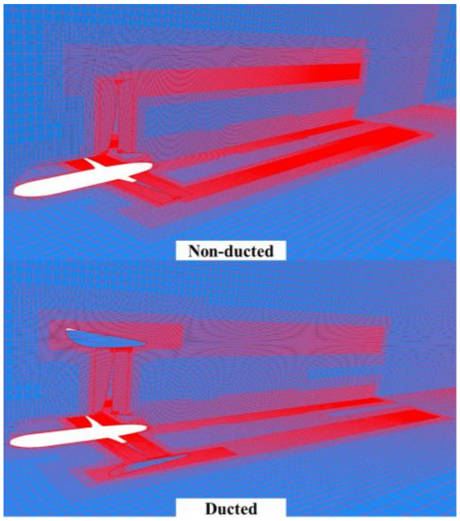

Fig.5 Mesh side view of ducted propeller

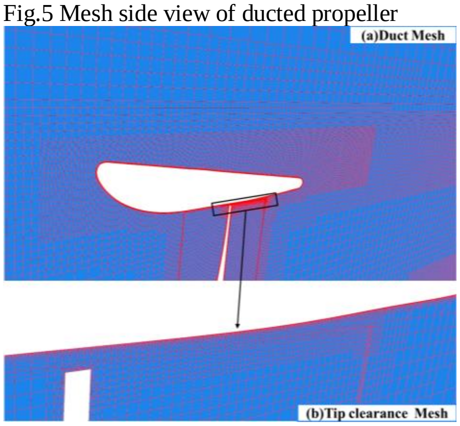

Fig.6 Duct and tip clearance mesh of the ducted propeller

RESULTS AND DISCUSSION

Open Water Characteristics

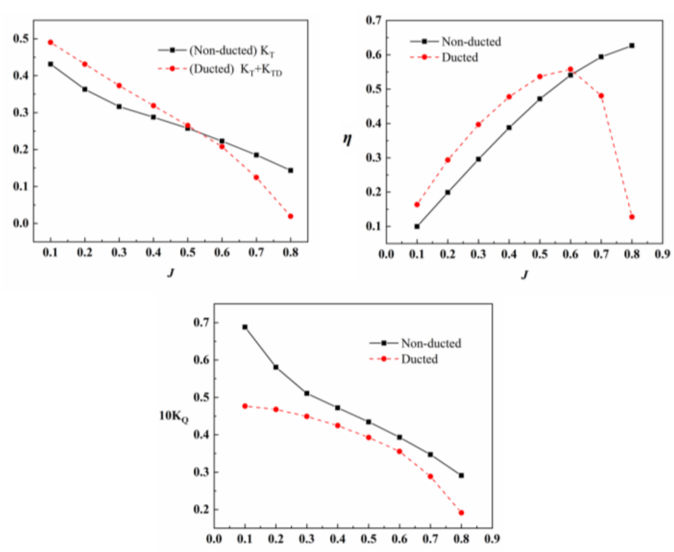

Fig.7 The open water characteristics results of non-ducted and ducted propeller

The open water performance of non-ducted and ducted propeller is simulated, and the comparison of the open water performance is shown in the Fig 7. The results show that compared with the open water propeller, K_{TD} is a new item, which provides a higher overall propulsion at low speeds, and therefore improves the efficiency of ducted propeller at low advance coefficient (J<0.61). At higher speeds, the K_{TD} of the duct becomes worse, so the overall force drops quickly, which shows that this type of ducted propeller is suitable for low-speed conditions and provides additional thrust. Moreover, the value of K_Q of ducted propeller is smaller than that of non-ducted propeller at all advance coefficients, which is related to the effect of the duct on the tip vortex, it reduces the torque on the blade.

Flow Characteristics in Wake

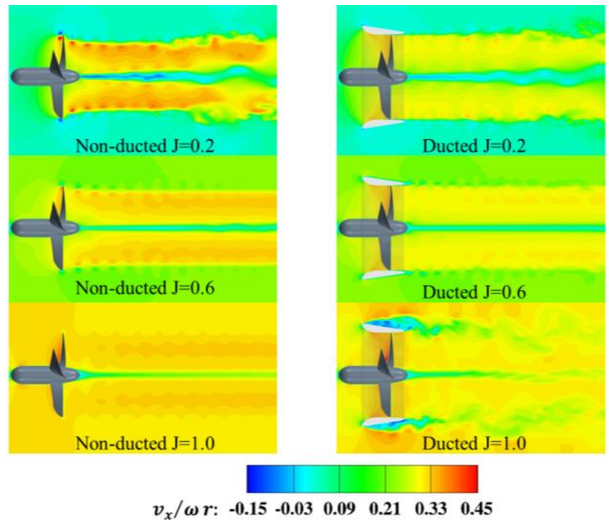

Fig.8 Axial velocity coefficient in wake of non-ducted and ducted propeller

The axial velocity of wake is captured and the rotation speed is used for dimensionless. The result is shown in Fig 8. On the whole, the duct can widen the wake area behind the propeller and make its velocity distribution more uniform. At low advance coefficients, the effect of duct on improving wake stability is particularly obvious. At the same time, the presence of the duct slows down the interaction between the hub vortex and the blade tip vortex, which is also one of the reasons for the improved wake stability.

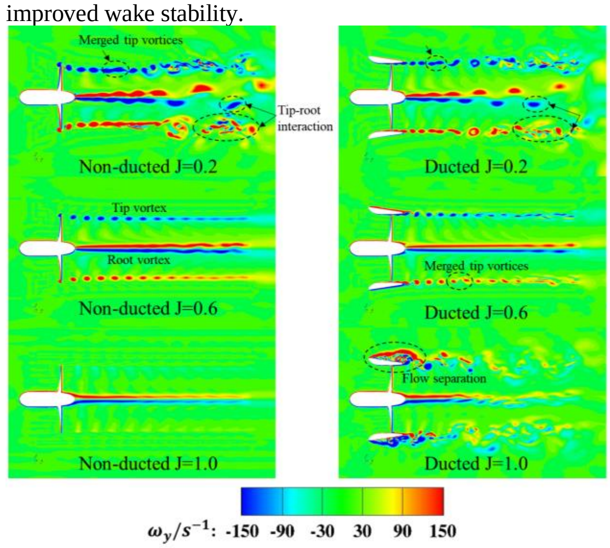

Fig.9 Vorticity-y in wake of non-ducted and ducted propeller

The comparison of wake vorticity, namely, the curl of field velocity, whose components in the y direction between the ducted and non-ducted propellers (Fig.9) shows that the presence of the ducted can reduce the instability of the wake vorticity at the low advance velocity coefficient, make the vortex distribution in the tail uniform, and slow down the interaction between the tip vortex and the axial vortex. In the case of high advance coefficient, there are a large number of vortices on the outer surface of the duct. Due to the extreme intensification of the duct vortices, the existence of such a duct increases the instability of the wake, which is inappropriate, indicating that the 19A duct is not suitable for high advance coefficient.

Tip Vortex Dynamics

The wake vortices of ducted propeller is captured by $Q = 5000\ s^{-2}$ at $J = 0.2$, $Q = 1500 s^{-2}$ at $J = 0.6$ and 1.0, and the result is shown in the Fig 10~12. Q represents the physical quantity of one of second generation vortex identification methods, and it is defined as:

$$Q = -\frac{1}{2}\left[\left(\frac{\partial u}{\partial x}\right)^2 + \left(\frac{\partial v}{\partial y}\right)^2 + \left(\frac{\partial w}{\partial z}\right)^2 + 2\frac{\partial u}{\partial y}\frac{\partial v}{\partial x} + 2\frac{\partial u}{\partial z}\frac{\partial w}{\partial x} + 2\frac{\partial v}{\partial z}\frac{\partial w}{\partial y}\right] \quad (10)$$

At low advance coefficient (in Fig10), there are a large number of secondary vortices in the wake of the non-ducted propeller, and the merger of the two vortices is serious, while the secondary vortices in the wake of the ducted propeller are relatively few, and the mutual inductance of the two vortices is light.

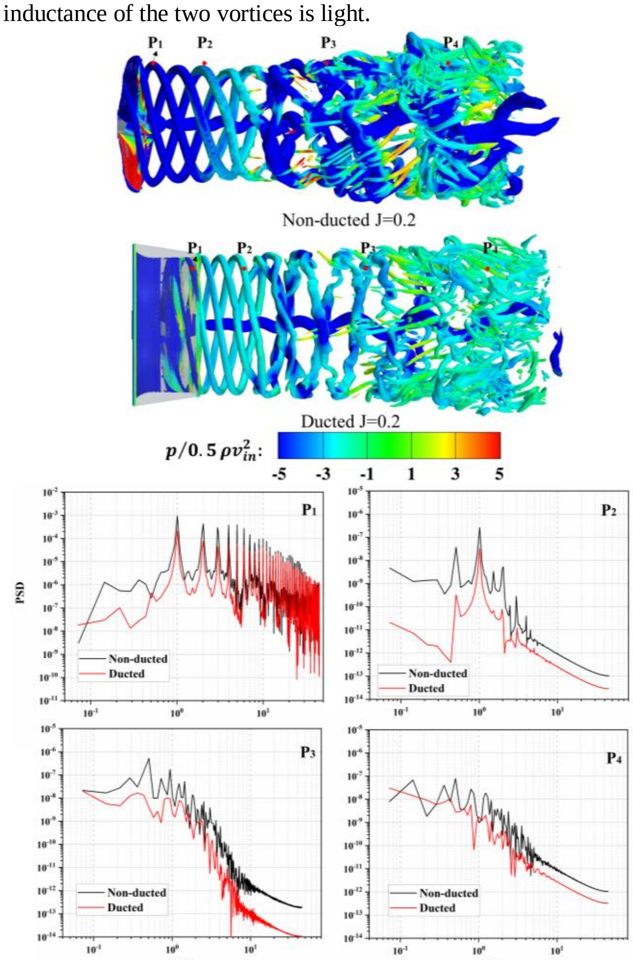

Fig.10 Vortex and instability in wake of non-ducted and ducted propeller when $J = 0.2$

At the same time, according to power Spectrum analysis (PSD), the peak values of non-ducted propeller at points P1 to P4 were higher than those of ducted propeller, which indicated that 19A duct could optimize the wake of Ka4-70 propeller and reduce their wake instability at a low advance coefficient. Especially when $J = 0.2$, the mutual inductance merging of adjacent tip vortices will occur in the wake of the propeller. The existence of the duct reduces this phenomenon and improves the stability of the wake.

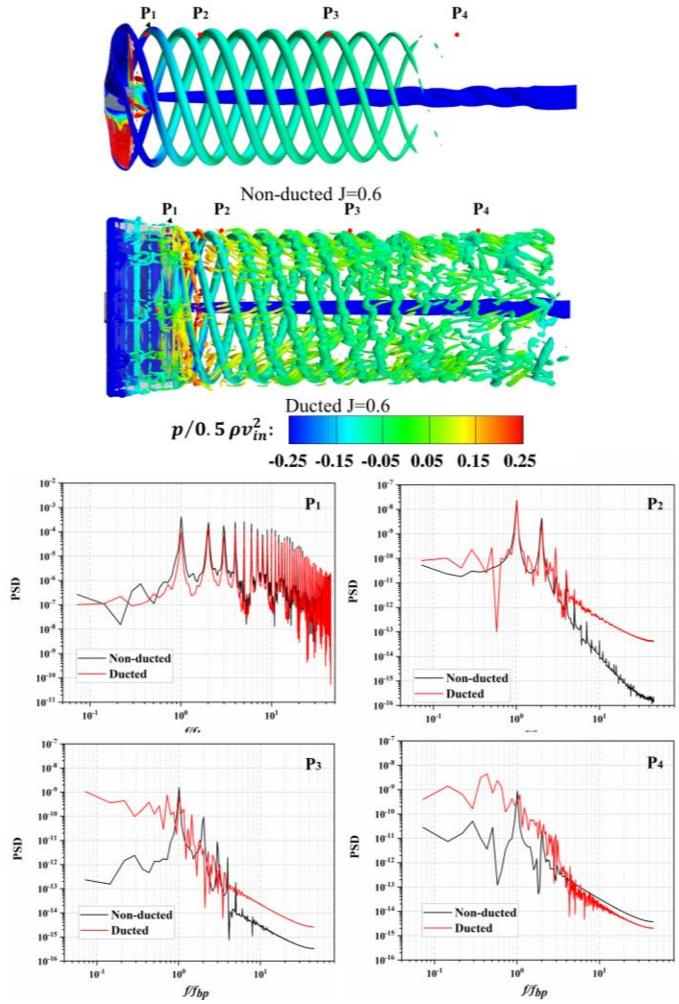

Fig.11 Vortex and instability in wake of non-ducted and ducted propeller when $J = 0.6$

Under middle advance coefficient (in Fig.11), namely $J = 0.6$, the wake of non-ducted propeller is gentle, while the wake vortex system of ducted propeller has many secondary vortices, which may enhance the instability of the wake. Furthermore, PSD analysis shows that at the P1 measurement point in Fig.11, both the ducted propeller and the non-ducted propeller have obvious peaks in the blade passing frequency and its multiplier, but the peak value of the ducted propeller is relatively small, which indicates that such 19A duct can still reduce the energy in the near-field wake under the medium advance coefficient, thus improving the energy recovery rate. However, at the P2-P4 measurement points in Fig.11, except for the peak position where the value of the ducted propeller is lower than that of the non-ducted propeller, the value of other parts of ducted propeller is higher, indicating that under this condition, compared with the non-ducted propeller, the vortex in the wake of such type of 19A duct takes the lead to instability.

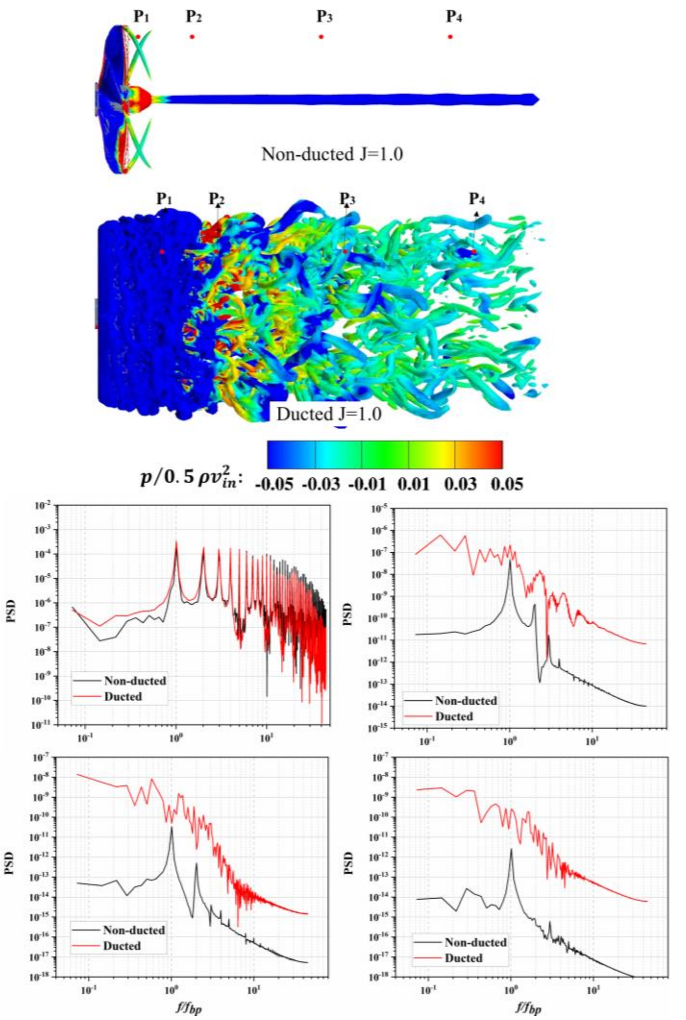

Fig.12 Vortex and instability in wake of non-ducted and ducted propeller when J = 1.0

Under high advance coefficient, the wake of non-ducted propeller is relatively gentle, while the ducted vortex system of the ducted propeller is more obvious, which greatly increases the energy loss and instability of the wake. PSD analysis shows that at P1-P4 measurement points in Fig.12, The energy peak value and the general value of the ducted blade are higher than that of the non-ducted blade, which is due to the serious flow separation of the ducted blade at the high advance coefficient, resulting in a large amount of energy waste. It means that this type of 19A duct is not suitable for very high speed.

CONCLUSIONS

Based on the detached eddy simulation (DES) turbulence modelling method, three advance coefficients J =0.2, 0.6 and 1.0 were simulated. The influence of the duct on vortex structures was analyzed in detail. The results show that additional thrust is provided by duct at low advance coefficients, but the thrust and efficiency of ducted propellers are reduced at higher advance coefficients, indicating that this type of duct is not suitable for high advance coefficients. The simulation of J = 0.2, 0.6, 1.0 shows that the duct can effectively improve the stability of the vortex structure at low advance coefficients, but it is no longer applicable at higher advance coefficients.

ACKNOWLEDGEMENTS

This work is supported by National Natural Science Foundation of China (Nos. 52001210, 52131102, 51879159), the Oceanic Interdisciplinary Program of Shanghai Jiao Tong University (SL2020PT104), to which the authors are most grateful.

REFERENCES

Cao, LS., Huang, FL., Liu, C., Wan, DC. (2021). Vortical Structures and Wakes of a Sphere in Homogeneous and Density Stratified Fluid. Journal of Hydrodynamics. 33(2), 207-215.

Carlo, N (2015). "Prediction of the performance of ducted propellers with BEM and hybrid RANS-BEM methods," *Faculty of Mechanical, Maritime and Materials Engineering (3mE)-Delft University of Technology*.

Celik, C. (2019). A methodology to predict the thrust-reduction, 18th International Congress of the Maritime Association of the Mediterranean, Varna, Bulgaria.

Felli M, Camussi R, Di Felice F. (2011). Mechanisms of evolution of the propeller wake in the transition and far fields. *Journal of Fluid Mechanics*, 682: 5-53.

Gaggero, S., Villa, D., Tani, G., Viviani, M., Bertetta, D., 2017. Design of ducted propeller nozzles through a RANSE-based optimization approach. Ocean Engineering. 145, 444-463.

Gong, J., Ding, J., Wang, L., 2021. Propeller–duct interaction on the wake dynamics of a ducted propeller. Physics of Fluids. 33 (7).

Heydari, M, Sadat-Hosseini, H (2020). Analysis of propeller wake field and vortical structures using k−ω SST Method, Ocean Engineering, 204, 107247.

Hughes, M. J., Kinnas, S. A., and Kerwin, J. E. (1992). "Experimental Validation of a Ducted Propeller Analysis Method." ASME. J. Fluids Eng. June 1992; 114(2): 214–219.

Li, H, Huang, Q, Pan, G (2021). Wake instabilities of a pre-swirl stator pump-jet propulsor. *Physics of Fluids*, 33(8): 085119.

Menter, F (1993). "Zonal two equation *k-ω* turbulence models for aerodynamic flows,"2*4th Fluid Dynamics, Plasmadynamics, and Lasers Conference*, 2906.

Menter, F (1994). "Two-equation eddy-viscosity turbulence models for engineering applications," *AIAA J.* 32(8), 1598-1605.

Qin, D, Huang, Q, Pan, G. (2021). Numerical simulation of vortex instabilities in the wake of a preswirl pumpjet propulsor. *Physics of Fluids*, 33(5): 055119.

Song, B., Wang, Y., Tian, W. (2015). Open water performance comparison between hub-type and hubless rim driven thrusters based on CFD method. Ocean Engineering. 103, 55-63.

Spalart, P. R., Deck, S., Shur, M. L., Squires, K. D., Strelets, M. K., & Travin, A. (2006). A New Version of Detached-eddy Simulation, Resistant to Ambiguous Grid Densities. *Theoretical and Computational Fluid Dynamics*, *20*(3), 181-195.

Wang, LZ, Guo, CY, Xu, P, and Su YM (2019). Analysis of the wake dynamics of a propeller operating before a rudder, *Ocean Engineering*, 188, 106250.

Wang, LZ, Wu, TC, and Guo, CY (2021). Study on instability mechanism and evolution model of propeller tip vortices. *Chinese Journal of Theoretical and Applied Mechanics*, 53(8): 2267-2278

Zhang, XD, Cao, LS, Wan, DC, and Shi FF. (2021). "Prediction of Open Water Performance of a Ducted Propeller by RANS and DES Methods." Paper presented at the The 31st International Ocean and Polar Engineering Conference, Rhodes, Greece.